ISSN 1063-7834, Physics of the Solid State, 2016, Vol. 58, No. 3, pp. 481–484. © Pleiades Publishing, Ltd., 2016.
Original Russian Text © L.T. Denisova, L.G. Chumilina, K.A. Shaikhutdinov, G.S. Patrin, V.M. Denisov, 2016, published in Fizika Tverdogo Tela, 2016, Vol. 58, No. 3, pp. 469–472.

DIELECTRICS

Heat Capacity and Thermodynamic Properties of $HoMnO_3$ in the Range of 364–1046 K

L. T. Denisova[a], L. G. Chumilina[a], K. A. Shaikhutdinov[a,b], G. S. Patrin[a,b], and V. M. Denisov[a]

[a] *Siberian Federal University, Svobodnyi pr. 79, Krasnoyarsk, 660041 Russia*

[b] *Kirensky Institute of Physics, Siberian Branch of the Russian Academy of Science, Akademgorodok 50, Krasnoyarsk, 660036 Russia*

e-mail: antluba@mail.ru

Received August 18, 2015

Abstract—The temperature dependence of the molar heat capacity of $HoMnO_3$ has been measured by differential scanning calorimetry. The experimental data have been used to calculate the thermodynamic properties of the oxide compound (changes in the enthalpy $H°(T) - H°(364\ K)$, entropy $S°(T) - S°(364\ K)$, and reduced Gibbs energy $\Phi°(T)$). The data on the heat capacity of $HoMnO_3$ have been generalized in the range of 40–1000 K.

DOI: 10.1134/S1063783416030070

1. INTRODUCTION

In recent years, researchers' interest in orthomanganites of rare-earth elements $RMnO_3$ (R = La–Lu, Y) has not declined [1–6]. Their magnetic and structural properties are well studied. At the same time, their thermodynamic properties have not yet been adequately studied. Currently, the data on the heat capacity are available mostly for low temperatures: $ScMnO_3$, $YMnO_3$, $LuMnO_3$ (0–200 K) [7]; $YMnO_3$, $HoMnO_3$, $ErMnO_3$, $TmMnO_3$, $LuMnO_{3+\delta}$ (0–150 K) [8]; $SmMnO_3$ (298–1500 K) [9]; $LaMnO_{3+\delta}$ (30–200 K) [10]; $LaMnO_3$ (77–760 K) [11]; $YMnO_3$ and $YbMnO_3$ (298–1373 K) [12]; $HoMnO_3$ (2–100 K) [13, 14]; $ErMnO_3$ (2–100 K) [14]; and $HoMnO_3$ (2–300 K) [15]. However, even the available data on the heat capacity at low temperatures differ rather significantly. As an example, such data are shown in Fig. 1 for $HoMnO_3$. At the same time, to optimize the synthesis conditions and to refine phase equilibria by thermodynamics methods, the data on thermodynamic properties of such compounds at high temperatures are required.

The objective of this work is to experimentally study the high-temperature heat capacity of $HoMnO_3$ and to determine its thermodynamic properties by these data.

2. SAMPLES AND EXPERIMENTAL TECHNIQUE

The $HoMnO_3$ crystals for measuring the heat capacity were grown using an FZ-T-4000-H optical floating-zone melting setup (Crystal Systems Corp., Japan). The samples obtained were analyzed by X-ray diffraction using a X'Pert Pro MPD diffractometer (PANalytical, Netherlands) with CoK_α radiation. Measurements were performed using a PIXcel fast detector with a graphite monochromator in the angular range of 10°–115° with a step of 0.013°. The data obtained are shown in Fig. 2. The lattice parameters were determined by full-profile refinement by the derivative difference minimization method [16].

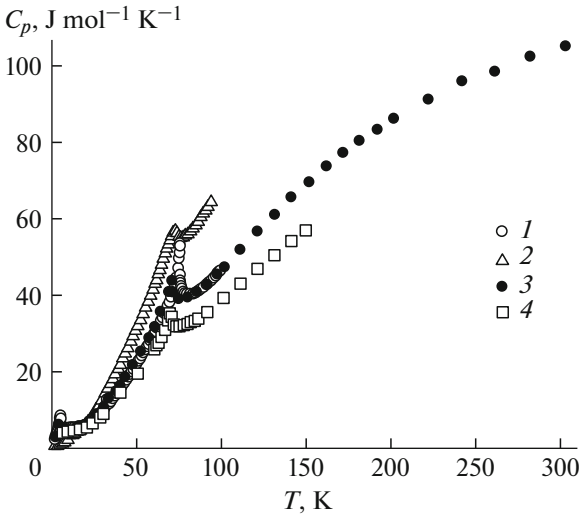

Fig. 1. Effect of the temperature on the low-temperature heat capacity of $HoMnO_3$: (*1*) data of [13], (*2*) [14], (*3*) [15], and (*4*) [8].

Table 1. Unit cell parameters of $HoMnO_3$

a, Å	c, Å	References
6.13	11.43	[1]
6.142(3)	11.417(7)	[2]
6.135	11.414	[3]
6.1493	11.4165	[14]
6.1406(1)	11.4340(3)	Our data

These values for $HoMnO_3$, in comparison with the results of other studies, are given in Table 1.

We can see that the parameters of synthesized oxide compound $HoMnO_3$ (space group $P6_3cm$, V = 373.37(1) Å^3) are in good enough agreement with the available data.

The molar heat capacity of $HoMnO_3$ was measured by the differential scanning calorimetry method (STA 449 C Jupiter, NETZSCH) in the temperature range of 364–1046 K. Platinum crucibles and special holders for measuring the heat capacity were used in the experiments. The measurement technique is similar to that described previously [17, 18]. The experimental data were processed using the NETZCSH Proteus Thermal Analysis package.

3. RESULTS AND DISCUSSION

The effect of the temperature on the molar heat capacity of $HoMnO_3$ is shown in Fig. 3. We can see a distinct extremum in the dependence $C_p = f(T)$ in the range of 583–801 K. The continuous variation in the heat capacity in the region of the extremum allows us to speak of a second-order phase transition, and the λ-shaped heat capacity peak suggests that thermodynamic fluctuations affect the heat capacity of $HoMnO_3$ near the phase transition. The temperature of the heat capacity maximum is T_{max} = 659 K. The heat capacity jump in the phase transition region is $\Delta C_p(T_{max}) \approx 3$ J mol^{-1} K^{-1}, and the transition width is $\Delta T \approx 208$ K.

It may be noted that the curve of the temperature dependence of the permittivity contains an extremum whose position is close to that in the dependence $C_p = f(T)$ [14].

The extremum in the curve $C_p = f(T)$ was previously observed for manganite $LaMnO_3$ [3, 11] in the region of 735 K.

The presence of such extrema is quite often related to the ferromagnet–paramagnet phase transition at the Curie temperature T_C [19, 20]. The value of T_C for various manganites $RMnO_3$ is in the range of 590–1000 K [13, 14]. According to various data for $HoMnO_3$, the Curie temperature is 830 [13] and 875 K [14, 21]. We obtained such a difference in T_C and the data of [13, 14] is not unexpected, since it is known that the critical temperature, as a rule, does not coincide with heat capacity C_p and magnetic susceptibility maxima [19, 22].

Disregarding the excess heat capacity associated with the phase transition, the dependence $C_p = f(T)$ for $HoMnO_3$ can be described by the classical Maier–Kelley equation [23] (in the units of J mol^{-1} K^{-1})

$$C_p = a + bT + cT^{-2} = (126.21 \pm 0.25) + (6.6 \pm 0.2) \times 10^{-3} T - (19.30 \pm 0.29) \times 10^5 T^{-2}. \quad (1)$$

The correlation coefficient for Eq. (1) is 0.9992.

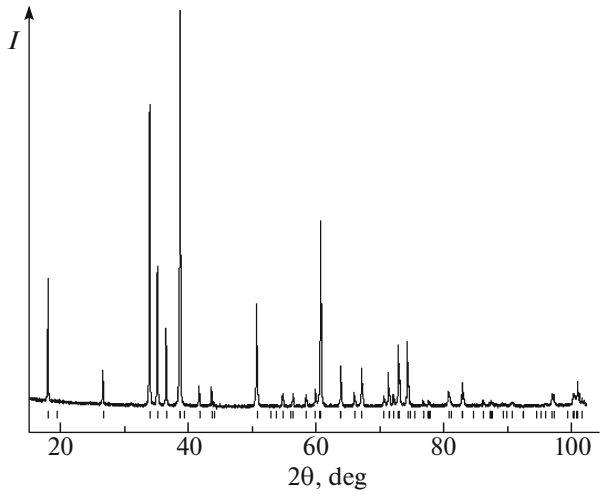

Fig. 2. X-ray diffraction pattern of $HoMnO_3$ at room temperature.

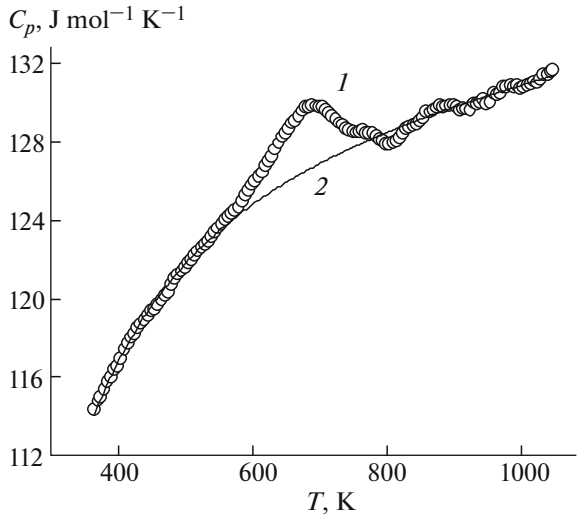

Fig. 3. Temperature dependence of the molar heat capacity of $HoMnO_3$: (*1*) experiment and (*2*) calculation by Eq. (1).

Table 2. Thermodynamic properties of $HoMnO_3$

T, K	C_p, J mol^{-1} K^{-1}	$H°(T) - H°$ (364 K), kJ mol^{-1}	$S°(T) - S°$ (364 K), J mol^{-1} K^{-1}	$\Phi°(T)$, J mol^{-1} K^{-1}
364	116.3	–	–	–
400	118.2	4.22	11.06	0.50
450	120.4	10.19	25.12	2.47
500	122.1	16.25	37.89	5.38
550	123.5	22.39	49.59	8.88
600	124.6	28.60	60.38	12.73
650	125.6	34.85	70.40	16.78
700	126.6	41.16	79.75	20.95
750	127.4	47.51	88.51	25.16
800	128.2	53.90	96.76	29.38
850	129.0	60.33	104.6	33.58
900	129.7	66.80	111.9	37.73
950	130.3	73.30	119.0	41.82
1000	131.0	79.83	125.7	45.85

Using relation (1), the changes in the enthalpy $H°(T) - H°(364\ K)$, entropy $S°(T) - S°(364\ K)$, and reduced Gibbs energy $\Phi°(T)$ were calculated by the known thermodynamic equations. The results are given in Table 2.

Figure 4 shows the data on the heat capacity of $HoMnO_3$ obtained in the present study (364–1000 K) and in [15] (3–300 K). We can see good agreement of these results. It was found that, without regard to phase transitions, the dependences $C_p = f(T)$ can be described by one general equation [24]

$$C_p = k_0 + k\ln T + k_1T^{-1} + k_2T^{-2} + k_3T^{-3}, \qquad (2)$$

which for the temperature range of 40–1000 K is written as

$$C_p = 308.40 - 22.02\ln T - 27.31\times10^3T^{-1} + 13.57\times10^5T^{-2} - 2.43\times10^7T^{-3}. \qquad (3)$$

The correlation coefficient for Eq. (3) is 0.9997.

It follows from Eq. (3) that C_p for $HoMnO_3$ at 298 K is 105.7 J mol^{-1} K^{-1} which is close to the value obtained for $ErMnO_3$ in [25] (104.8 J mol^{-1} K^{-1}).

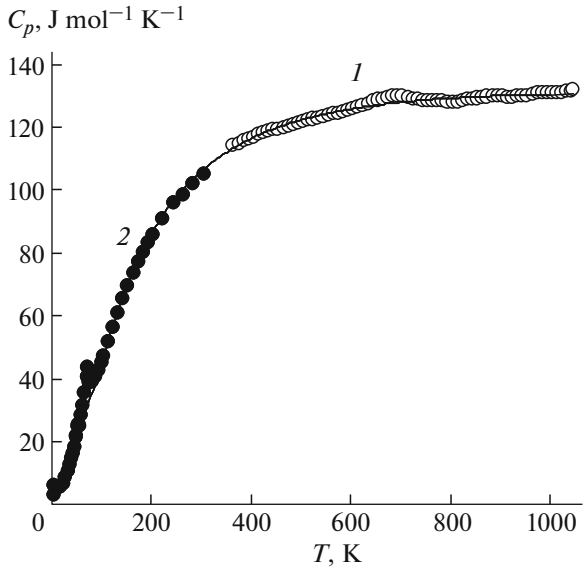

Fig. 4. Effect of the temperature on the heat capacity of $HoMnO_3$: (*1*) data of this study, (*2*) data of [15]; the solid line is the calculation by Eq. (3).

The heat capacitys C_p^0 for $HoMnO_3$ are calculated by the Neumann–Kopp method [26],

$$C_p^0(HoMnO_3) = \frac{1}{2}C_p^0(Mn_2O_3) + \frac{1}{2}C_p^0(Ho_2O_3). \qquad (4)$$

The heat capacitys of initial oxides, required for calculation by Eq. (4), are taken from [26]. It was found that in this case $C_p^0(HoMnO_3) = 0.47$ J g^{-1} K^{-1}, which is higher than the experimental value 0.40 J g^{-1} K^{-1}. This confirms the data of [27] that the Neumann–Kopp equation usually yields overestimated values of C_p^0 in comparison with experimental values.

4. CONCLUSIONS

The high-temperature heat capacity of $HoMnO_3$ (364–1046 K) was measured. It was found that the dependence $C_p = f(T)$ contains a small extremum at

T_{max} = 659 K. Thermodynamic properties of the oxide compound were determined.

REFERENCES

1. V. E. Wood, A. E. Austin, E. W. Colings, and K. C. Brog, J. Phys. Chem. **34**, 859 (1973).
2. H. W. Brinks, H. Fjellvåg, and A. Kjekshus, J. Solid State Chem. **129**, 334 (1997).
3. A. N. Grundy, M. Chen, B. Hallstedt, and L. J. Gauckler, J. Phase Equilib. Diffus. **26** (2), 131 (2005).
4. S. Remsen and B. Dabrowski, Chem. Mater. **23**, 3818 (2011).
5. C. N. R. Rao, A. Sundaresan, and R. Saha, J. Phys. Chem. Lett. **3**, 2237 (2012).
6. S. M. Selbach, A. N. Lovik, K. Bergum, J. R. Tolchard, and M.-A. Einarsud, J. Solid State Chem. **196**, 528 (2012).
7. D. G. Tomuta, S. Ramakrishnan, G. J. Neiwenkuys, and J. A. Mydosh, J. Phys.: Condens. Matter **13**, 4543 (2001).
8. C. Fan, Z. Y. Zhao, J. D. Song, J. C. Wu, F. B. Zhang, and X. F. Sun, J. Cryst. Growth **388**, 54 (2014).
9. E. Pawlas-Foryst, K. T. Jacob, and K. Fitzner, Arch. Metall. Mater. **51** (2), 253 (2006).
10. L. Ghivelder, I. A. Castilo, M. A. Gusma[tilde]o, J. A. Alonso, and L. F. Cohen, Phys. Rev. B: Condens. Matter **60**, 12184 (1999).
11. H. Saton, M. Takagi, K.-I. Kinukawa, and N. Kamegashira, Thermochim. Acta **299**, 123 (1997).
12. H. Saton, J.-I. Iwasaki, K. Kawase, and N. Kamegashira, J. Alloys Compd. **268**, 42 (1998).
13. B. Lorenz, F. Yen, M. M. Gospodinov, and C. W. Chu, Phys. Rev. B: Condens. Matter **71**, 014438 (2005).
14. P. Liu, X.-L. Wang, Z.-X. Chen, Y. Du, and H. Kimura, Phys. Rev. B: Condens. Matter **83**, 144404 (2011).
15. A. Midya, S. N. Das, P. Mandal, S. Pandya, and V. Ganesan, Phys. Rev. B: Condens. Matter **84**, 235127 (2011).
16. L. A. Solovyov, J. Appl. Crystallogr. **37**, 743 (2004).
17. L. T. Denisova, L. G. Chumilina, N. V. Belousova, and V. M. Denisov, Russ. J. Phys. Chem. A **89** (8), 1335 (2015).
18. V. M. Denisov, L. T. Denisova, L. A. Irtyugo, and V. S. Biront, Phys. Solid State **52** (7), 1362 (2010).
19. A. G. Gamzatov, A. M. Aliev, K. Sh. Khizriev, I. K. Kamilov, A. S. Mankevich, and I. E. Korsakov, Phys. Solid State **53** (11), 2271 (2011).
20. V. M. Denisov, L. T. Denisova, L. A. Irtyugo, G. S. Patrin, N. V. Volkov, and L. G. Chumilina, Phys. Solid State **54** (11), 2205 (2012).
21. N. N. Loshkareva, A. S. Moskvin, and A. M. Balbashov, Phys. Solid State **51** (5), 930 (2009).
22. S. V. Vonsovskii, *Magnetism* (Nauka, Moscow, 1971; Wiley, New York, 1974).
23. C. G. Maier and K. K. Kelley, J. Am. Chem. Soc. **54** (8), 3243 (1932).
24. P. Richet and G. Fiquet, J. Geophys. Res., B **96** (1), 445 (1991).
25. H. Satoh, T. Shoji, J. Iwasaki, and N. Kamegashira, Thermochim. Acta **261**, 47 (1995).
26. J. Leitner, P. Chuchvalec, D. Sedmidubský, A. Strejc, and P. Abrman, Thermochim. Acta **395**, 27 (2003).
27. L. T. Denisova, Yu. F. Kargin, and V. M. Denisov, Phys. Solid State **57** (8), 1699 (2015).

Translated by A. Kazantsev